

Ultra-fast Diagnostics of Laser-induced Melting of Matter in ns to μ s Time-scales

Alexander HORN*, Ilja MINGAREEV* and Isamu MIYAMOTO**

* *Lehrstuhl für Lasertechnik der RWTH Aachen, Steinbachstrasse 15, 52074 Aachen, Germany*

** *Osaka University, 2-1, Yamada-Oka, Suita, Osaka 565-0871, Japan*

E-mail: alexander.horn@ilt.fraunhofer.de

The interaction of laser radiation with dielectrics and metals is detected with femtosecond resolution by pump&probe techniques ($t = 80$ fs or 3 ps, $\lambda = 810$ nm). Even with femtosecond laser radiation melt ejection dynamics can be observed by irradiating metals like copper or aluminium using time-resolved shadowgraphy. Laser-induced melt ejection has been observed in the time range of 100 ns to 1.04 μ s after the initial laser-metal interaction. Depending on metal-specific parameters, rosette-like surface structures of the ablated regions are observed.

The modification of BK7 glass by femtosecond or picosecond laser radiation is observed by time-resolved Nomarski-Photography using ultra-short pulsed white-light continuum as probe beam. The pump beam is focussed by a microscope objective into the glass. After partial absorption of the optical energy the glass is heated and depending on the focus diameter ($2\omega_0 \approx 1$ μ m) cracking is induced. For BK7 glass using picosecond laser radiation modification and cracking are induced. By decreasing the intensity of the laser radiation glass can be melted inside and on the surface without cracking.

Keywords: ablation, modification, delay line, melt ejection, high-speed photography, pump&probe

1. Introduction

The interaction of femtosecond laser radiation with different materials is intensively studied, because femtosecond laser radiation gives two major advantages to micro-machining compared to nanosecond and longer pulses: (i) the reduction of the pulse energy which is necessary to induce ablation for fixed laser wavelength and focusing conditions, and (ii) a significant reduction of heat-affected zone (HAZ) and, as consequence, the improvement of the contour sharpness for the laser-processed structures. The second advantage is a direct consequence of the pulse duration being much smaller than the heat diffusion time of metals and dielectrics. Improved availability and compactness of ultra-short, sub-ps pulsed solid-state lasers has stimulated a growing interest in the exploiting of the enhanced flexibility of femtosecond technology for industrial micro-machining. Numerous materials like metals [1][2], semiconductors [3], ceramics [4], dielectrics [5] and composite materials [6] have been investigated. However, many aspects of the femtosecond ablation remain unclear, while the regimes of the processing of some industrially important materials are not yet optimized.

The interaction of ultra-short laser radiation with matter is accompanied by processes like heating, melting and plasma formation for metals and optical breakdown, avalanche ionization, multi-photon ionization or color center formation for dielectrics [7][8]. The interaction of laser

radiation with dielectrics can be divided into three main process regimes: absorption, optical emission, and modification. Irradiation with femtosecond laser radiation can induce melting without cracking: wave guides can be generated by focusing the laser radiation inside glasses, inducing a refractive index change [9][10][11].

Ultra-fast time-resolved optical shadowgraphy and Nomarski-Photography combine pump-probe technique with optical microscopy, allowing time- and space-resolved measurements of the changes in the material morphology induced by the laser excitation pulse. A low-loss multi-pass optical delay stage enabling time delays up to 1.2 μ s and preserving small pulse duration of the probe laser radiation is presented. In this work, some of the characteristics resulting from femtosecond laser interaction with metals and glasses will be elucidated by means of direct visualization techniques such as time-resolved shadowgraphy and Nomarski-Photography.

2. Laser and Measurement tools

Laser ablation experiments on metal surfaces and dielectrics were performed using a femtosecond time-resolved pump-probe setup (Fig. 1) to image the emission of particles, vapor and melt after irradiation on the surface of metals by shadowgraphy and to image refractive index changes inside dielectrics by Nomarski-Photography. The temporal resolution of the focused beam is measured with an autocorrelator (APE Mini) and is given by the duration of the

probe pulse, typically around 100 fs. The spatial resolution is determined by the properties of the imaging optics, e.g. numerical aperture and magnification, and can be of the order of a micrometer. Generally, the temporal detection region is technically limited by the delay stage used in the experimental setup. A femtosecond CPA-laser system (Thales Concerto) operated in single pulse mode up to 1.5 mJ per pulse at the wavelength $\lambda=810\text{-}820$ nm, spectral bandwidth $\Delta\lambda = 25$ nm (FWHM), and pulse duration t_p in the range 80 fs - 3 ps with nearly Gaussian beam of $M^2 = 1.5$ was used.

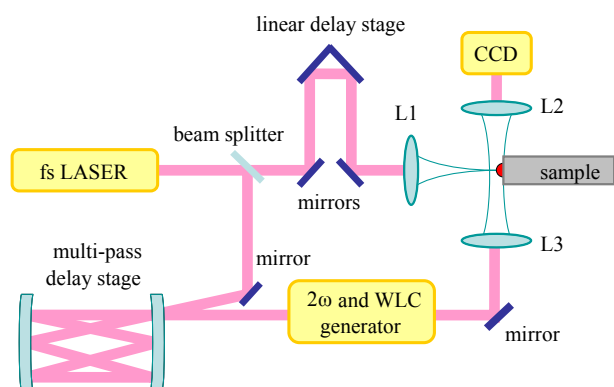


Fig. 1 Schematic setup of the femtosecond and picosecond pump&probe experiment.

For the investigations on metals the laser radiation is focused by a microscope objective L1 (Olympus MSPlan20, NA = 0.4) to a calculated spot size of about $10\ \mu\text{m}$ with a magnification of 20x. The applied pulse energy constitutes up to six times the ablation threshold for each metal under investigation. After a beam splitter, the laser radiation passes a low-loss multi-pass optical delay stage [15] and a 2ω or white light continuum (WLC) generator, forming a probe beam (L2, L3) that is perpendicular to the optical axis of the pump laser radiation. By adjusting the multi-pass delay stage on an optical rail and by use of an additional linear delay stage for the pump laser radiation, the length of the optical paths of the pump and probe beams can be continuously varied resulting in an overall delay time of $1.2\ \mu\text{s}$. About $10\times 10\times 1\ \text{mm}^3$ sized, polished Al or Cu samples with optical quality surfaces featuring high chemical purity (>99.9%) are flexibly moved by three high-precision stages (PI Physikinstrumente). Shadow-graphs are taken by a CCD camera (Baumer Optronic arc4000c), using a microscope objective L2 (Olympus MSPlan50, NA = 0.55) with the overall spatial resolution of $1.5\ \mu\text{m}$. Ex-situ measurements of the induced surface morphology are performed with scanning electron microscopy (SEM).

The investigations on modification in polished BK7 glass with optical quality (size $10\times 10\times 1\ \text{mm}^3$) are performed using the above described CPA Ti:Sapphire femtosecond laser. Using Nomarski-Photography the modification by heating of the glass matrix and the generation of a sound wave has been observed. The set-up for pump&probe Nomarski-Photography with a variable delay ($t = 0 - 66$ ns) is described elsewhere [33][34]. The output beam is divided into two beams by a beam-splitter. The

exciting beam is focused by a microscope objective (Olympus MSPlan50, NA = 0.55) within the substrate $300\ \mu\text{m}$ below the surface and a WLC probe beam irradiates perpendicular to the pump beam the interaction zone.

3. Results and Discussion

3.1 Plasma and melt dynamics of metals

In general, the interaction of high power pulsed laser radiation with solid materials involves complex phenomena, e.g. of optical, thermal, mechanical or hydrodynamic nature. During the first instants of the interaction the incident energy is distributed among these phenomena. For the investigations on metals, using ultra-fast laser radiation in the near-infrared wavelength range, linear and two-photon absorption is assumed to be dominant absorption mechanisms [16][17][18]. A part of the initial energy is absorbed leading to the heating of the bulk. Then, the melting and the vaporization of the irradiated sample can be observed.

Energetic electrons overcoming the work function of the metal can escape from the target. Consequently, the electric field created by the charge separation between the escaping electrons and parent ions effectively could pull ions out of target [19][20]. Thus, the energetic fast ions [21] are likely emitted via a non-thermal process during the early stage of ablation in the time range up to some nanoseconds. It should be noted, however, that the net surface charge density due to non-thermal process was reported to be two orders of magnitude lower than in dielectric materials [22]. Gradual increase in absorption of the irradiated area was observed at small elapsed times $\tau < 3.0$ ns due to the emergence of a thin plasma layer in the proximity of the sample surface that attenuates the reflected probe laser beam used for diagnostics.

The plasma and melt dynamics can be described qualitatively well with some well-known theoretical issues [23] based on the molecular dynamics assumptions. In this experiment, however, to be contrary to the performed calculations, significant differences in the time-scales of dynamic processes can be observed due to unlike focusing conditions and different applied pulse energy. According to the theoretical and experimental data on ablation dynamics of solids [24][25], the expansion starts with a rarefaction wave that proceeds from the surface into the material. After reflection at the unperturbed substrate the rarefaction wave travels towards the surrounding atmosphere. This results in a thin layer of high density, which is moving away from the target in front of a low density region. The low density region is assumed to be a liquid-gas mixture caused by homogenous nucleation within a few tens of picoseconds.

Theoretical and experimental works on ablation mechanisms of metals and semiconductors on nanosecond for time-scales and longer by evaporation and “normal boiling” effects after heterogeneous nucleation have been reported [26][27]. Calculations [28] performed for metals above the boiling temperature, however, result in a removal of only several atom layers in 100 ns. Therefore, this process seems to be negligible for short timescales. Concerning boiling effects, heterogeneous nucleation in the liquid is involved. Calculations for metals at twice the melting temperature result in diffusion distances $< 1\ \text{nm}$ in 100 ns. Therefore, normal boiling is also not expected to have sig-

nificant contribution to the ablation for the time scale $<1 \mu\text{s}$. Experiments on GaAs below the plasma formation threshold [25], however, show bubble-like structures in the liquid. These bubbles appear about 20 ns after the ablation pulse and grow linear in time.

Qualitative differences of the performed surface modifications in copper and aluminium (Fig. 2 a and b) occurred. The surface morphology of copper reveals rosette-like modifications. Solidified melt droplets and material jets on sub-micrometer size scale can be seen in the distance of some 5-10 μm from the center of the ablated region. Slightly elliptical contours of the produced craters correspond to the spatial beam profile of the used laser radiation. In contrast to that, the crater contours on aluminium targets retain sharp edges. The heat conductivity of metals is coupled to the electron-phonon-coupling constant resulting in a complex hydrodynamic movement of the melt. Besides the similar optical properties of copper and aluminum smaller values of the electron-phonon-coupling constant for copper ($\mu_{\text{Cu}} = 10 \cdot 10^{16} \text{ W m}^{-3} \text{ K}^{-1}$ and $\mu_{\text{Al}} = 4.1 \cdot 10^{16} \text{ W m}^{-3} \text{ K}^{-1}$) result in a larger amount of melt when irradiating copper with ultra-short laser radiation.

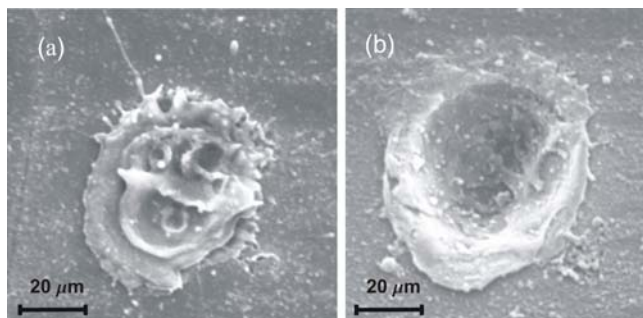


Fig. 2 Surface structures induced in Cu (a) and Al (b) by single pulse ultra-fast laser radiation (SEM, $\lambda = 820 \text{ nm}$, $t_p = 80 \text{ fs}$, $F = 0.3\text{-}0.4 \text{ J/cm}^2$).

In this paper the dynamics of the melt formation and material ablation for single pulse irradiation at larger pump-to-probe elapsed times up to $\tau = 1.2 \mu\text{s}$ (Fig. 3) reveals a variety of phenomena, like plasma formation, ejection of material droplets and liquid jets [15]. The experimental data shows that the phenomenological development of the ablation dynamics on the time delay range between $\tau = 3.0 \text{ ns}$ and $\tau = 1.04 \mu\text{s}$ can be conditionally categorized into three characteristic time regions. The first one features photo-induced emission, formation and expansion of highly pressurized, heated material, combined with the beginning formation of shock waves (Fig. 3 a and b). At the time delay $\tau = 49 \text{ ns}$ (Fig. 3 a) an expanding shock wave can be observed. The expansion of shock wave and vapor plume in gas can be described by a combined model developed for nanosecond ablation [26][27].

At approximately $\tau = 200 \text{ ns}$ time delay (Fig. 3 c and d), the ablated material is ejected explosively. Observation of ejected droplets and material particles with dimensions (approx. 1 – 3 μm) can be measured for the investigated metals Cu and Fe and can be related to the aforementioned nucleation and boiling effects [26][27][28].

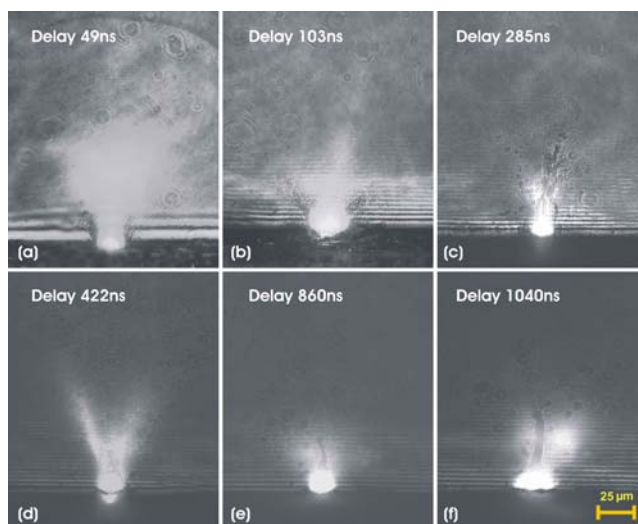


Fig. 3 Shock wave, plasma and melt emitted from Al as function of time delay (Shadowgraphy, $F = 1.8 \text{ J/cm}^2$, $\lambda_{\text{pump}} = 820 \text{ nm}$, $t_p = 80 \text{ fs}$, WLC).

During the third characteristic time region at time delays $\tau > 700 \text{ ns}$ (Fig. 3 e and f), a jet of molten material expanding vertically upward with a velocity of about 100 m/s was observed on aluminium targets. The estimated height of the ejected structures averages about 50 μm at the delay $\tau = 1.04 \mu\text{s}$. This transient melt ejection can be compared qualitatively, with respect to different absorption and heat conduction in bulk compared to thin films, to the works on nano-jets and micro-bumps formation on gold films by Korte et al. being carried out at comparable fluences [25]. Because of the similar thermal properties and similar small electron-phonon coupling constants of aluminium and gold ($\mu_{\text{Al}} = 4.1 \cdot 10^{16} \text{ W m}^{-3} \text{ K}^{-1}$ and $\mu_{\text{Au}} = 2.3 \cdot 10^{16} \text{ W m}^{-3} \text{ K}^{-1}$) melt is formed. Contrary to the experiments of Korte et al. the experiments were carried out well above ablation threshold: the generated melt structures do mostly not result in permanent micro-bumps.

3.2 Plasma and melt dynamics of glasses

The involved processes when ultra-fast-laser radiation interacts with dielectrics are manifold: starting by a quasi-instantaneous multi-photon absorption of laser radiation by bounded electrons free electrons are generated. A competing absorption is due to defects in non-ideal dielectrics, which have lower band gap. These highly excited electrons relax by interacting with other free-electrons and with the phonons of the dielectric material heating up the bulk [30]. The relaxing electrons generate different defects, like self-trapped excitons [31] and color centers [32]. Borosilicate glass have been excited with laser radiation at fixed pulse energy ($E_p = 0.1$ and 5 μJ) and pulse duration ($t_p = 80 \text{ fs}$ and 3 ps) with the position of the sound wave [33][34] and the width of the modification measured.

After absorption of the radiation due to multi-photon or defect-absorption the free electrons relax forming defects and/or heating up the glass. An optical emission of the plasma can be detected for about 10 ns. Modification and strong cracking induced by picosecond are observed at the pulse energy 5 μJ for the investigated material in the excitation volume. The cracking starts during the first 1-2 ns

and shows typical cracking near the irradiation zone (Fig. 4 a). All the cracks formed in the investigated materials show larger dimensions when irradiated by picosecond laser radiation. Cracking induced by femtosecond laser radiation cannot be detected (Fig. 4 b). Even after 66 ns the glass is still hot and the modification can be detected due to the modified refractive index (Fig. 4 c). Reducing the pulse energy to $0.1 \mu\text{J}$ a transient modification in both glasses can be observed up to 66 ns (Fig. 4 d), but no permanent modification. This observable reversible modification is due to heating and consequent refractive index change of the glass.

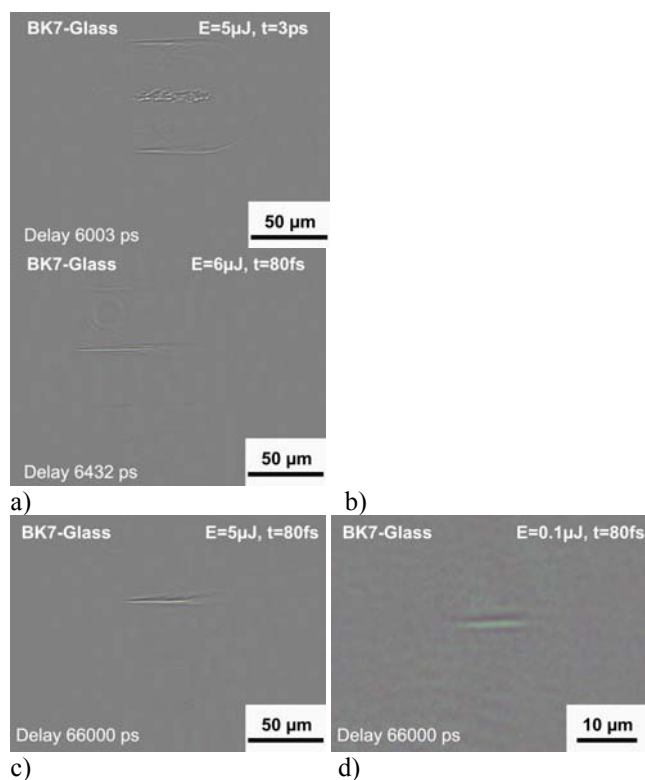


Fig. 4 Modification and cracking after 6 ns (a,b) and 66 ns (c,d) in BK7 glass (Nomarski -Photography, $\lambda = 810 \text{ nm}$, $t_p = 80 \text{ fs}$ and 3 ps , $I = 241 \text{ TW/cm}^2$ and $I = 9.05 \text{ PW/cm}^2$).

The sound wave propagates at sound velocity (about 6 km/s) cylindrically to the beam propagation direction (Fig. 5). The width of the modified glass increases in some tens of picoseconds. Irradiating the glass with laser radiation at $t_p = 3 \text{ ps}$ pulse duration and at $5 \mu\text{J}$ pulse energy the expansion of the modification takes about 5 to 10 ps (inset Fig. 5). This increase in width is partially due to the spatial and temporal intensity distribution (so called isophote) of the laser radiation in the focus. The modification width increases within 10 ns to about $10\text{--}12 \mu\text{m}$ due to melting and cracking.

4. Conclusion

A novel pump-probe setup designed and deploying a low-loss multi-pass optical delay stage, enables time-resolved observation of modification and ablation up to $\tau = 1.2 \mu\text{s}$ after the irradiation of the sample with high temporal ($> 100\text{fs}$) and spatial resolution ($> 1 \mu\text{m}$).

Shadowgraphs provide direct visualization of plasma development and melt ejection dynamics on the time scale up to $1.04 \mu\text{s}$ after the initial laser-material interaction. Being in accordance with some theoretical issues on ablation by ultra-short laser radiation, observed ablation dynamics implies processes with emission of particles, vapour and melt up to several hundred nanoseconds after the laser pulse in at least three characteristic time regions. The phenomenology during the first ablation stage includes expansion of highly pressurized, heated material up to 200 ns after the material irradiation. An explosion-like emission of melt droplets with diameter smaller than $3 \mu\text{m}$ can be observed at delays up to 700 ns, which has been also reported by some groups. Finally, a massive melt ejection at time delays larger than approximately 700 ns with velocities up to 100 m/s occurs.

The modification of BK7 glass irradiated by ultra-fast laser radiation shows modification due to heating. A reversible modification is observed up to 66 ns, whereas an irreversible modification is found at pulse energies $\geq 1 \mu\text{J}$. The modification width after irradiation with picosecond laser radiation increases within 5-10 ps to about $10 \mu\text{m}$. Cracking is observed for pulse energies above $1 \mu\text{J}$ and a pulse duration of 3 ps. The development of sound waves and modification due to melting in borosilicate glass gives indication for a propagating velocity of about 6 km/s cylindrically and perpendicular to the beam propagation.

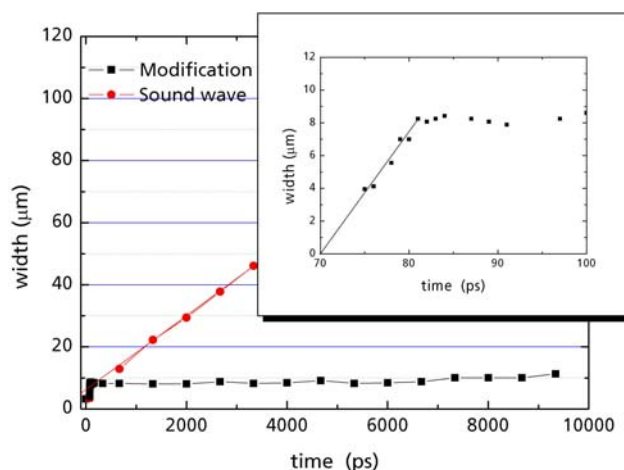


Fig. 5 Width of sound wave and modification as function of time for BK7 glass with inset describing the width of the modification as function of time close to creation ($\lambda = 810 \text{ nm}$, $t_p = 3 \text{ ps}$, $I = 241 \text{ TW/cm}^2$).

References

- [1] N.N. Nedialkov, S.E. Imamova, P.A. Atanosov, Ablation of metals by ultrashort laser pulses, *J. Phys. D: Appl. Phys.*, **37**, (2004) 638.
- [2] P. Mannion, J. Magee, E. Coyne, G.M. O'Connor, Ablation thresholds in ultrafast laser micro-machining of common metals in air, *Proceedings SPIE*, **4876**, (2003) 470.
- [3] J.Krüger und W.Kautek, Femtosecond-pulse laser processing of metallic and semiconducting thin films, *Proceeding SPIE*, **2403**, (1995) 436.

- [4] J. Ihlemann, A. Scholl, H. Schmidt, B. Wolff-Rottke, Nanosecond and femtosecond excimer laser ablation of oxide ceramics, *Appl. Phys. A*, **60**, (1995) 411.
- [5] S. Campbell, F.C. Dear, D.P. Hand, D.T. Reid, Single-pulse femtosecond laser machining of glass, *J. Opt. A*, **7**, (2005) 162.
- [6] J. Krüger, W. Kautek, Femtosecond pulses visible laser processing of fibre composite materials, *Appl. Surf. Sci.*, **106**, (1996) 383.
- [7] R.R. Alfano, (1989) *Supercontinuum Laser Sources*, Springer-Verlag, Berlin Heidelberg.
- [8] R.R. Alfano & Shapiro, S.L., Observation of Self-Phase Modulation and Small-Scale Filaments in Crystals and Glasses, *Phys. Rev. Lett.*, **24**, (1970) 592-594.
- [9] K.Miura, J. Qui, H. Inouye and T.Mitsuyu and K.Hirao, photowritten optical waveguides in various glasses with ultrashort pulse laser, *Appl. Phys. Lett.*, **71**, (1997) 3329-3331.
- [10] A. Saliminia, N.T. Nguyen, R. Vallee, Writing optical waveguides in fused silica using 1kHz fs infrared pulses, *J. of Appl. Phys.*, **93**, (2003) 3724-3728.
- [11] M. Will, S. Nolte, B. Chichkov, A. Tünnermann, Optical properties of waveguides fabricated in fused silica by femtosecond laser pulses, *Appl. Opt.*, **41**, (2002) 4360-4364.
- [12] T. Tamaki, W. Watanabe, J. Nishii and K. Itoh, Welding of Transparent Materials Using Femtosecond Laser Pulses, *Jap. J. of Appl. Phys.* **44** (2005) L 687–L 689.
- [13] D. Wortmann, M. Ramme, J. Gottmann, Volume waveguides by refractive index modification using fs-laser double pulses and ps-laser radiation, Proc. of the 4th International Congress on Laser Advanced Materials Processing LAMP 2006, Kyoto (2006), to be published.
- [14] I. Miyamoto, A. Horn, J. Gottmann, Local melting of glass material and its application to direct fusion welding by ps-laser pulses, Proc. of the 4th International Congress on Laser Advanced Materials Processing LAMP 2006, Kyoto (2006), to be published.
- [15] I. Mingareev, A. Horn, E.W. Kreutz, Observation of melt ejection in metals up to 1 μ s after femtosecond laser irradiation by a novel pump-probe photography setup, Proc. of SPIE, International Conference on High-Power Laser Ablation, Taos, (2006) to be published.
- [16] R. Hermann, J. Gerlach, and E. Campbell, Ultrashort pulse laser ablation of silicon: an MD simulation study, *Appl. Phys. A*, **66**, (1998) 35.
- [17] N. N. Nedialkov, S E Imamova and P A Atanasov, *J. Phys. D: Appl. Phys.* **37** (2004) 638—643
- [18] L. Zhigilei, Dynamics of the plume formation and parameters of the ejected clusters in short-pulse laser ablation, *Applied Physics A*, **76** (2004) 339
- [19] Tae Y. Choi and Costas P. Grigoropoulos, Plasma and ablation dynamics in ultrafast laser processing of crystalline silicon, *J. of Appl. Phys.* **92**, (2002) 9
- [20] M. Ye and C. P. Grigoropoulos, *J. Appl. Phys.* **89**, (2001) 5183
- [21] F. Dausinger, F. Lichter and H. Lubatschowski, *Femtosecond Technology for Technical and Medical Applications*, Springer, Heidelberg (2004).
- [22] R. Stoian, A. Rosenfeld, D. Ashkenasi, I. V. Hertel, N. M. Bulgakova and E. E. B. Campbell, Surface Charging and Impulsive Ion Ejection during Ultrashort Pulsed Laser Ablation, *Phys. Rev. Lett.*, **88**, (2002) 097603.
- [23] Danny Perez and Laurent J. Lewis, Ablation of Solids under Femtosecond Laser Pulses, *Phys. Rev. Lett.*, **89**, (2002) 255504.
- [24] K. Sokolowski-Tinten, J. Bialkowski, A. Cavalleri, M. Boing, H. Schüler and D. von der Linde, Dynamics of femtosecond laser induced ablation from solid surfaces, *Proc. SPIE*, **3343**, (1998) 46.
- [25] K. Sokolowski-Tinten, J. Bialkowski, M. Boing, A. Cavalleri and D. von der Linde, Bulk phase explosion and surface boiling during short pulse laser ablation of semiconductors, *OSA Technical Digest*, **231** (1999).
- [26] J. König, S. Nolte and A. Tünnermann, Plasma evolution during metal ablation with ultrashort laser pulses, *Optics Express*, **13**, No. 26, (2005) 10597.
- [27] D. Bäuerle, *Laser Processing and Chemistry*, 3rd ed., (2000).
- [28] R. Kelly and A. Miotello, Contribution of vaporization and boiling to thermal-spike sputtering by ions or laser pulses, *Phys. Rev. E*, **60**, (1999) 2616.
- [29] F. Korte, J. Koch, B.N. Chichkov, Formation of microbumps and nanojets on gold targets by femtosecond laser pulses, *Appl. Phys. A*, **79**, (2004) 879.
- [30] P.N. Saeta, B.I. Greene, Primary Relaxation Processes at the Band Edge of SiO₂, *Phys. Rev. Lett.*, **70**, (1993) 3588-3591.
- [31] W. Joosen, S. Guizard, P. Martin, G. Petite, P. Agostini, A. Dos Santos, G. Grillon, D. Hulin, A. Migus, A. Antonetti, Femtosecond Multiphoton Generation of the Self-Trapped Exciton in α -SiO₂, *Appl. Phys. Lett.*, **61**, (1992) 2260-2262.
- [32] S. Guizard, M. Meynardier, Time-Resolved Study of Laser-Induced Color Centers in SiO₂, *J. Phys. of Condens. Matter*, **8**, (1996) 1281-1290.
- [33] A. Horn, H. Khajehnouri, E.W. Kreutz, R. Poprawe, Time Resolved Optomechanical Investigations on the Interaction of Laser Radiation with Glass in the Femtosecond Regime, Proc. of LIA, **94**, (2002) 1577-1585.
- [34] A. Horn, H. Khajehnouri, E.W. Kreutz, R. Poprawe, Ultrafast Pump and Probe Investigations on the Interaction of Femtosecond Laser Pulses with Glass, Proc. of SPIE, **4948**, (2002) 393-400.
- E. W. Kreutz, A. Horn, R. Poprawe, Electron Excitation in Glasses and Sapphire Followed by Time- and Space-Measuring Tools, Proc. of SPIE, **5620**, (2004) 239-244.

(Received: May 16, 2006, Accepted: December 9, 2006)